FINAL PROJECT SUMMARY REPORT

PROJECT IDENTIFICATION INFORMATION

1. BUSINESS FIRM
Prime Research, LC
1750 Kraft Dr Ste 1000-B
Blacksburg, VA 24060

2. DOT SBIR PROGRAM: 2004 PHASE I

3. DOT CONTRACT NUMBER: DTRS57-04-C-10012

4. PERIOD OF PERFORMANCE: From 23 Dec 2003 To 23 June 2004

5. PROJECT TITLE: Intrinsic Distributed in Fiber Optic Leak Detection

SUMMARY OF COMPLETED PROJECT

Monitoring and inspection of pipelines are essential for optimal operation of the energy infrastructure of the nation. However, methods that are currently used for pipeline inspection and diagnostics are typically either slow, do not provide high spatial resolution, suffer from excessive false-alarms, or are not real-time. For this Phase I SBIR program, Prime Research investigated the application of a new photonic sensor technology to detection and monitoring of acoustic waves, such as those that may result from leaks in gas pipelines. Two new innovations were explored: the manufacturing of intrinsic Fabry-Perot interferometer (IFPI) sensors in an optical fiber using a UV laser, and the use of an Optical Time Domain Reflectometer (OTDR) to interrogate Fabry-Perot sensors.

Significant progress was achieved in the fabrication of IFPI sensors using the UV laser. While the first sensors made suffered low mechanical strength and poor optical performance (fringe visibility), improvements to the fabrication process yielded mechanically robust sensors with good fringe visibility. However, tests of the IFPI sensors for detection of acoustic stress waves in a metal plate and a metal pipe indicated that the sensors are less sensitive than alternative interferometric sensors, such as extrinsic Fabry-Perot sensors. The lower sensitivity is attributed to the stiffness of the all-glass IFPI assembly.

Experimental evaluation of a commercial high-resolution OTDR for Fabry-Perot sensor interrogation indicated that this method is poorly suited for monitoring of acoustic signals. In order to achieve reasonable signal-to-noise ratios, the optical signal must be heavily averaged, reducing the effective signal bandwidth to frequencies much less than that required for acoustic monitoring. In addition, a large noise amplitude in the OTDR resulted in poor resolution. It was found that than alternative interferometric sensor interrogation system, the Self Calibrating Interferometric/Intensity Based (SCIIB) system, yielded much better signal to noise ratio than the OTDR, and did not require signal averaging, resulting in a higher signal bandwidth.

APPROVAL SIGNATURES

1. PRINCIPAL INVESTIGATOR 2. PRINCIPAL INVESTIGATOR 3. DATE

Russell G. May

1 Research Objectives

The technical objectives for the program were:

Objective 1 – Identify characteristic acoustic signatures that will enable the fiber optic distributed intrinsic sensors to positively identify leaks in a multiphase pipeline. This will establish both the system level requirements and the sensor level performance metrics.

Objective 2 – Determine the optimum sensor network and decoding system that will result in the most effective and economical optical leak detection. This will establish the best combination of sensor decoding and distribution techniques on the pipeline to maximize the detection probability for a leak and simultaneously minimize both hardware cost and lifetime operation expenditures.

Objective 3 – Establish preliminary system designs leading to Phase II and follow-on product commercialization. This will provide the basis for moving quickly to the product development stage.

2 Work Carried Out

The research carried out during the Phase I SBIR program is described in this section. Details regarding results of the research are given in the next section.

2.1 Description of tasks

The work performed during this program was organized into six tasks. The six tasks were:

Task 1 – Determine the metrics for acoustic detection in various pipeline installation modes.

Task 2 – Fabricate prototype fiber optic sensors with acoustic coupling mechanisms.

Task 3 – Adapt sensor decoding system to acoustic sampling methods.

Task 4 – Determine sensitivity of the fiber optic system using acoustic standards.

Task 5 – Extrapolate system performance and design a sensor network.

Task 6 – Prepare Phase I final report and Phase II program plan.

2.2 Background information

Optical fiber sensors, which have been extensively researched for twenty years, have been demonstrated to be useful for the measurement of a wide variety of physical and chemical parameters due to such inherent advantages as: 1) an immunity to electromagnetic interference, 2) avoidance of ground loops, 3) capability of responding to a wide variety of measurands, 4) avoidance of electric sparks, 5) resistance to harsh environments, 6) remote operation, 7) capability of multiplexing, and 8) ease of integration into large-scale fiber networking and communication systems. Sensors based on optical fibers can be made relatively inexpensively, since they may use fibers and optical components which have been developed and manufactured in large quantities to satisfy the booming market for optical communications.

A fiber optic sensor works by causing some change in the quality of the light wave launched into the fiber by a light emitting diode (LED) or laser diode. Some of the changes in the light wave that can be related to applied external effects include changes in intensity (optical power), wavelength, phase, and polarization.

For the development of a pipeline monitoring system, it was proposed to employ Fabry-Perot interferometric fiber sensors to monitor acoustic emissions resulting from leaks in the pipeline. Interferometry is an optical technique that measures changes in the phase of a light wave resulting from an applied measurand. In fiber optic Fabry-Perot acoustic sensors, stress waves are coupled into the optical fiber, resulting in any time-dependent elongation of the fiber in response to the acoustic signal. The elongation of the fiber results in a shift of the lightwave phase, which is detected by interferometric methods and related to the acoustic signal.

In the Fabry-Perot sensor, two reflecting surfaces are set up within the sensor fiber itself, producing local interference, the magnitude of which is related to the optical distance between the two reflectors, as shown in Figure 1. The two reflectors are often made from the flat ends of optical fibers, using the normal Fresnel reflections from the surfaces. The optical interference between the two reflected light waves sets up interference at the detector, which varies sinusoidally with the distance between the reflectors. These sinusoidal 'fringes' can be decoded to very accurately measure the distance between the fiber ends (the 'gap'). This is called an 'extrinsic' Fabry-Perot interferometer, or EFPI. By attaching the two fibers to a structure, any movement in the structure can be used to indirectly calculate the strain, or related parameters such as acoustic pressure.

The reliability of this type of sensor is questionable for long term performance, since the sensor is essentially a break in the fiber, and it is held together only by the capillary tube or other package device. The reflective surfaces inside the fiber can also be replaced by local changes in the refractive index, as shown in the lower portion of the figure. This is called an 'intrinsic' Fabry-Perot interferometric (IFPI) sensor. Prime Research, LC (PRLC) has an exclusive license on the technique developed by CPT to create the

changes by 'writing' them with a UV laser beam focused on the fiber core. IFPI sensors can be multiplexed by writing the spots into the fiber sequentially down its length, resulting in potentially thousands of sensors on a single fiber.

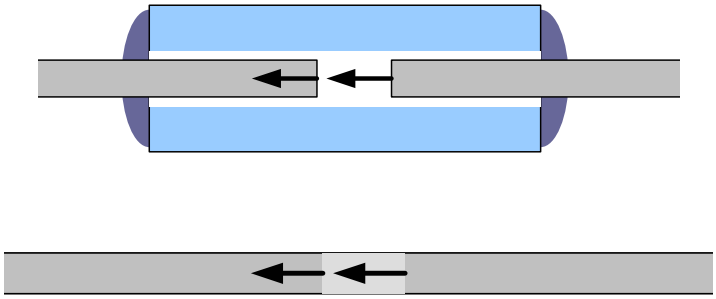

Figure 1. Extrinsic (top) and intrinsic (bottom) Fabry-Perot interferometric sensors.

The optical phase shift for a measurable disturbance such as a pressure wave generated by an acoustic signature is given by

$$\varphi = \frac{2\pi * 2L * n}{\lambda}$$

where L is the length of the Fabry-Perot cavity, n is the refractive index inside the cavity, λ is the wavelength of the light source. The change in phase Δφ is given by

$$\Delta\varphi = \frac{4\pi}{\lambda}(L * \Delta n + n * \Delta L)$$

This change is dependent upon L and n, and can be employed to approximate the anticipated cavity length.

2.2.1 Background on Fabry-Perot signal processing

There are several optical techniques that can be used to process the optical signal output by a Fabry-Perot fiber sensor, and convert the optical signal to an analog or digital electrical signal which is proportional to measurand (and acoustic stress waves, in this case). Two were investigated during this research: the Self-Calibrated Interferometric/Intensity Based (SCIIB) system, which is appropriate for single sensors, and the Optical Time Domain Reflectometer (OTDR) system, which is appropriate for multiple sensors multiplexed on a single fiber.

2.2.1.1 SCIIB

The sensor design was based on the breakthrough Self-Calibrated Interferometric/Intensity Based (SCIIB) optical sensor technology recently developed at Virginia Tech, and licensed by Prime Research for commercial development. This new approach to optical sensor design combines the best features of interferometric optical sensors, such as high sensitivity, with the best features of intensity-based optical sensors, such as simple signal processing and fast response times, without compromising the performance of either.

The SCIIB design embodies three innovations that make it well suited for acoustic measurements. First, an optical technique is used to provide self-calibration of the sensor, rendering it insensitive to undesired perturbations, such as fluctuation in source power or fiber cable loss. Secondly, the mechanical design of the sensor is adjusted so that the output (intensity) of the sensor is a linear function of the measurand, simplifying the processing of the sensor output. Thirdly, the use of organic adhesives such as epoxy is eliminated in the sensor construction, which may otherwise lead to viscoelastic creep in the sensor.

The operation of the SCIIB pressure sensor is illustrated in Figure 2. An optical source, such as a superluminescent diode, with a broad spectral output is connected through a 2x2 coupler to a sensor, which is formed by aligning the input fiber to a glass diaphragm with an optically reflective surface. A ceramic ferrule and a glass capillary tube are used to support the diaphragm. The end of the input fiber is cleaved or polished, so that a Fabry-Perot cavity is formed between the diaphragm and the fiber end. Two Fresnel reflections, R_1 and R_2 in the figure, are generated due to the difference in refractive indices of the glass and the air, and are guided back though the input fiber and the coupler to an optoelectronic subsystem where the optical signal is processed. In this subsystem, the optical signal is split into two paths: in one path, the full spectral width of the source is preserved, and in the second, the signal is optically filtered to reduce the spectral width.

Since the coherence length of a source or signal is inversely proportional to its spectral width, the channel with the reduced spectral width (Channel 2 in Figure 2) has a longer coherence length than the other channel. The bandpass of the optical filter in Channel 2 is chosen so that the resulting coherence length of that channel is greater than twice the length of the separation between the two fibers in the sensor. With that condition, interference between reflections R1 and R2 is observed in the output of the Channel 2 detector. Specifically, the output will vary sinusoidally with a change in the gap separating the sensor fibers. This change in the intensity of the light incident on the Channel 2 detector can be used to measure changes in the length of the air gap that may occur due to physical effects such as pressure.

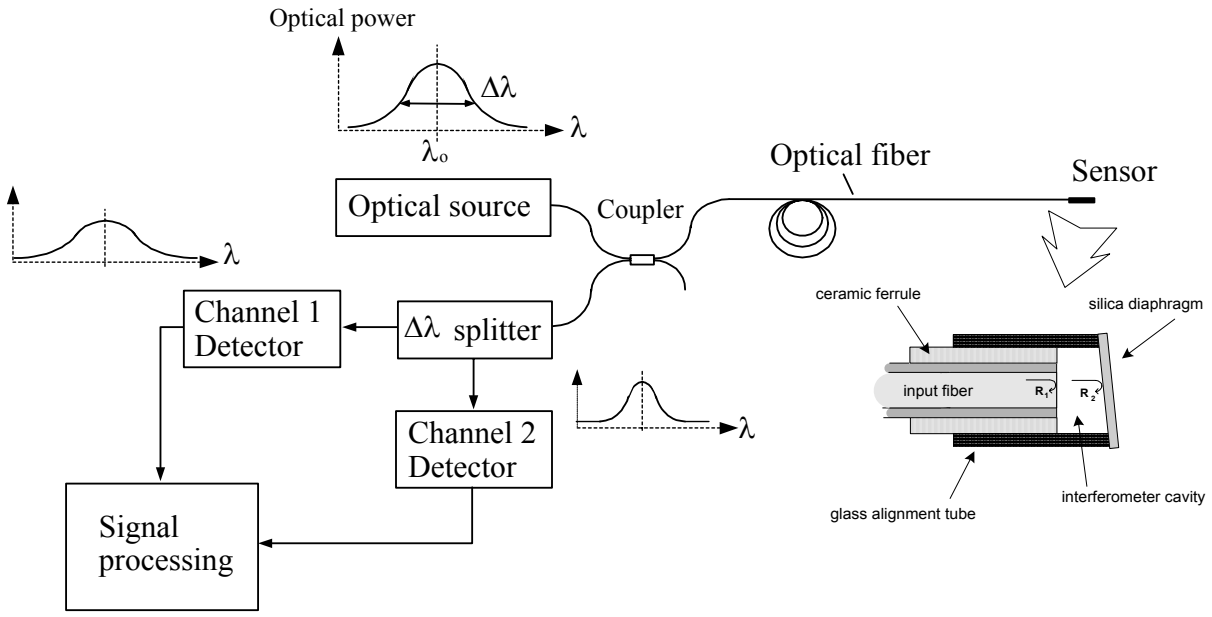

Figure 2. Schematic of Self-Calibrated Interferometric/Intensity-Based (SCIIB) Fiber Optic Sensor

To simplify the processing of the output signal, the construction of the sensor probe is adjusted in order to limit the output of Channel 2 to the quasi-linear region of the sensor output. Figure 3 illustrates the variation of optical intensity that results from the interference of reflections R1 and R2 when the gap separating the input fiber and the reflector fiber are increased. By choosing appropriate values for the thickness, diameter, and elastic modulus of the diaphragm, the output of the sensor over the desired operating range of the sensor can be constrained to fall within the region denoted by the blue line in Figure 3. The sensor output may then be interpreted as a linear function of the measurand; in this way, the simple signal processing of an intensity-based fiber optic sensor is achieved, with the high sensitivity characteristic of interferometric sensors.

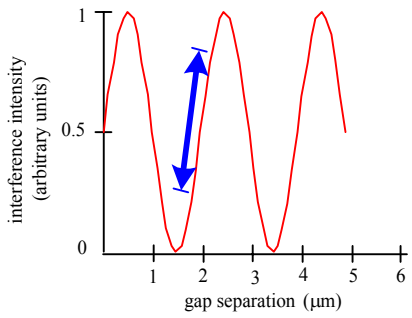

Figure 3. Output of Fabry-Perot interferometer, with quasi-linear output of sensor indicated by bold line.

If the output of the sensor is interpreted as a linear change in the output of Channel 2, then undesired physical effects that may change the intensity of light into the optoelectronic subsystem, such as fluctuations in the output power of the optical source or changes in the attenuation of the optical cable (due to bends, for instance) might be misinterpreted as a change in the parameter being measured. The second signal path in the optoelectronic subsystem (Channel 1 in Figure 2) is used to compensate for these undesired effects. Since light incident on the detector in that channel is unfiltered, it has that full spectral width of the source, and therefore has a short coherence length. During construction of the sensor probe, the gap between the two fibers is adjusted to ensure that it is longer than one half of the coherence length of Channel 1. In this way, the output of Channel 1 does not exhibit interference between the two reflections from the sensor; it is, however, proportional to the sum of the intensities of the two reflections. Changes in the source output power or in the cable attenuation or in connector loss are common mode to both channels, while the interference effects are exhibited only in Channel 2. Therefore, by taking the ratio of the output of Channel 2 to Channel 1, the undesired loss factors are canceled out, leaving only the factors describing the interference effects, which give the desired measurement.

2.2.1.2 OTDR

Optical Time Domain Reflectometry (OTDR) is an optical technique commonly used to find faults (breaks) in optical fiber cables. In OTDR, which is similar to an optical radar, a short optical pulse is launched into the sensor fiber (Figure 4). A small percentage of the pulse is reflected backwards by reflectors in the sensor elements. At the input of the sensor fiber, the reflected pulses are tapped off by a fiberoptic coupler, and are converted to an electrical signal by a photodetector and displayed on an oscilloscope. Since the speed of light in the fiber is known, the distances from the electronics to the reflectors can be calculated from the arrival time of the pulse at the detector. The intensity of the light reflected from each individual sensor can be determined from the display.

The use of OTDR to interrogate Fabry-Perot sensors was originally developed at the Center for Photonics Technology (CPT) at Virginia Tech. PRLC has an exclusive license to develop commercial products based on that innovation. PRLC has licensed exclusively from Virginia Tech a related technology that permits Intrinsic Fabry-Perot Interferometer (IFPI) cavities to be written into optical fibers using a high-powered UV laser.

In general, Fabry-Perot interferometers are formed by placing two parallel partially reflecting planar surfaces into the light path such that they are normal to the direction of light travel. While partially reflective surfaces can be constructed in a number of ways, CPT invented a unique way to place these surfaces within the existing fiber structure (hence, “intrinsic”) such that there are no parts to assemble. The two planar surfaces are formed by exposing a section of photo-sensitive fiber to ultraviolet laser light. As the section of fiber is exposed to the laser light, the index of the fiber core changes such that

it is different than that of the unexposed fiber. This index change creates partially reflecting surfaces at the two ends of the exposed section of fiber. This is very similar to the process used to create Fiber Bragg Gratings (FBG) in fiber; however, instead of creating a periodic pattern (many closely spaced small cavities) in the fiber as is done with FBGs, only one cavity, albeit longer in length, is written in the fiber.

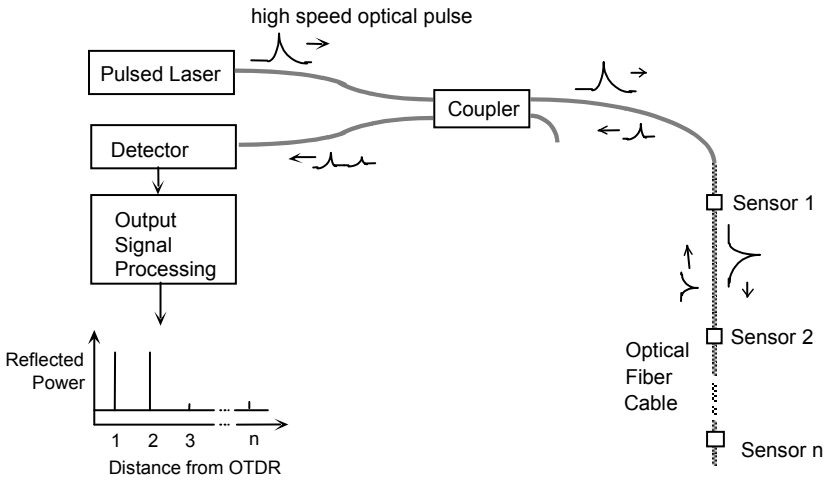

Figure 4. Schematic of OTDR system for interrogation of distributed sensors. Each sensor is an IFPI written in the fiber using an excimer laser.

As the light pulse from the OTDR propagates down the fiber, at each IFPI the two reflections interfere in the fiber, and are guided back to the input end of the fiber, where the state of interference may be analyzed using a photodetector. The state of interference (constructive or destructive) depends on the phase difference of the two reflections, which in turn is a function of the length of the cavity. If the sensor element is subjected to a change in temperature, the fiber length changes according to thermal expansion principles, resulting in a change in the state of interference. Alternately, by modifying the packaging of the sensor, any measurand, such as strain or pressure, that causes a change in the physical dimensions of the sensor package, may be measured.

The optical intensity output of the sensor varies sinusoidally with gap separation, as shown in Figure 3. The periodic variation of the intensity leads to an ambiguity in the determination of the gap separation. To eliminate this ambiguity, the length of the IFPI cavity and the mechanics of the sensor package are adjusted during fabrication such that the output of the sensor is limited to the linear part of the sensor output for the full anticipated range of the sensor operation, as shown by the bold line in Figure 3. In this way, the high sensitivity of the interferometric sensor is preserved, while the output can be processed as a simple intensity-based sensor, which is important to achieve multiplexing of a large number of sensor elements along a single fiber. Since the optical intensity of the light reflected from the sensor is now linearly dependent on cavity length,

an OTDR system can be used to analyze the reflected light and determine the cavity length from the intensity of the light reflected from each sensor. In addition, the OTDR may be used to measure Rayleigh backscatter in the fiber, which can be used to provide self-compensation of the sensor for variations in OTDR source power and optical fiber losses, as described below.

3 Results obtained

The results obtained during the Phase I SBIR research program are described in this section, and are organized according to task.

3.1 Task 1: Determination of metrics

In order to adopt design goals with a fiber-optic leak detection system, a study was undertaken to determine requirements for leak monitoring. This was accomplished using two strategies:

1. Prior industry experience with acoustic leak detection for pipelines utilizing electrical-based sensors was studied to determine whether acoustic signatures and their associated leak conditions were already known.

2. In order to focus our development efforts, industry statistics were explored to determine the type and size of pipe used, the leak geometries and scenarios that are the most problematic in the industry, the spatial resolution needed in leak detection, typical installation scenarios, and the perceived value of optical sensors over electrical sensors in this application.

There are two general types of leaks that are problematic for the pipeline industry – small leaks and large leaks. The large leaks are generally caused by catastrophic events caused by third party construction activities and are very easy to detect and locate without sensors as their damage is apparent. However, small leaks caused by corrosion represent the majority of the total leaks in gas transmission and are the most difficult to locate. For example, 44% of the leaks in transmission during 2002 were caused by corrosion while only 4% were caused by excavation. In addition, 99% of the leaks in gas transmission and gathering during 2002 occurred onshore. Thus, we will concentrate on the detection of small leaks in buried pipeline caused by corrosion.

After researching several patents and articles on the subject matter, we learned that the maximum acoustic frequency generated by a leak is around 100 kHz, with the majority of the energy below 40 kHz. This energy presents itself as white noise that is generally well below the energy generated by ambient conditions in the same spectral range such as normal gas flow in the pipe, wind, and pump noise. Advanced digital signal processing has been used in the past to identify and locate the leak by correlating the noise received at two or more sensors spatially distributed along the pipe. It has also been shown that the acoustic signature is very dependent on the pipeline dimensions, pipeline material,

and the type of soil that the pipeline is buried in. Our studies show that the majority (55%) of the installed pipe used for transmission and gathering is between 4" and 20" in diameter and is made of coated steel (96%). Previous tests also show that the acoustic signature is more dependent on the shape of the leak instead of the size of the leak. Our development will target the detection of leaks in the majority of the installed pipe and leak type.

The spatial resolution requirement for determining the location of a leak is highly dependent on the general location of the pipeline. For example, if the leak is in the middle of a cornfield, the pipeline company can afford to dig up a large portion of the field to find the leak. However, if the leak is in a metro area under a street, the leak detection needs to be accurate to within one or two feet. Given that the acoustic signatures for a leak are very small, the acoustic sensors need to be closely spaced down a pipe to detect a leak. Besides the fact that electrical sensors generally have a short lifetime when installed in the ground due to corrosion, the fact that they require power at closely spaced intervals on the pipeline is a major detriment for using electrical sensors as compared to optical sensors. There are times when the only available power along a pipeline is located at the pumps, typically located 60 miles apart. If wires are run along a pipeline to remote sensors, electrical noise generally overpowers the small acoustic signatures caused by leaks. The fiber optic sensors under development for this program will not be susceptible to EMI and will be designed such that they can be installed far away from available power sources.

3.2 Task 2: Fabricate sensors with acoustic coupling

Previous methods for the fabrication of intrinsic Fabry-Perot interferometric (IFPI) sensors, as described in the program proposal, suffered from several limitations. In that method, intense ultraviolet light from a KrF excimer laser irradiates a short length (a few hundred microns) of a photosensitive optical fiber, causing a small increase in the refractive index in the exposed section of the fiber. The discontinuities in refractive index between the exposed glass and the unexposed glass at the two ends of the exposed section form two weak reflectors, which define an optical cavity. The length of that optical cavity can be determined using any of several interferometry methods. Acoustic energy coupled into the optical fiber will modulate the length of the cavity, so that the output of the interferometer can be used to detect and monitor the acoustic signal.

The limitations of the previous method of fabricating the IFPI sensors were (1) fabrication of a given IFPI cavity length was difficult to reproduce, (2) damage to the fiber due to UV exposure resulted in a very low yield rate of usable sensors, due to the fragility of the exposed glass, and (3) the visibility (a measure of the interferometric fringe contrast which is related to the sensor signal-to-noise ratio) of the cavities was small (2-3 dB). All three of these difficulties were overcome during the research.

Reproducibility of a given cavity length was greatly improved by using a new "dual-exposure" technique to make the cavity. Previous efforts exposed the entire cavity length

to the UV laser output, as shown in Figure 5. The dual-exposure technique only exposes 20 um swathes at either end of the cavity length, illustrated in Figure 6. It is believed that this method is more repeatable because "hot-spots" in the excimer laser beam profile no longer create fluctuations in the refractive index of the cavity.

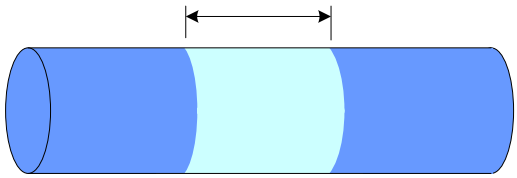

Figure 5. IFPI cavity written by a single UV exposure (light blue represents exposed glass).

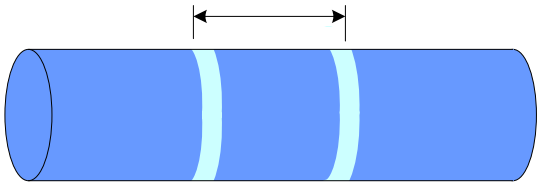

Figure 6. IFPI cavity written by dual-exposure method.

Microscopic examination of exposed fiber sections revealed that the high laser power was causing ablation of some of the glass around the circumference of the fiber, leading to stress concentration sites in the fiber. Physical damage to the fiber has been greatly reduced by careful manipulation of laser energy, beam focusing optics, and fixturing of the fiber. The recent cavities have shown very little damage and can be easily handled for further processing/packaging without fear of breaking the fiber.

Previous IFPI fringe visibility of 2-3 dB has been increased to 10-15 dB. It is believed that this improvement was achieved by changing the material used to construct the shutter blades which define the exposure aperture (Figures 7 and 8). The material was changed from stainless steel to silicon. This change resulted in sharper cavity definition and eliminated the oxidation and ablation problems associated with the steel blades.

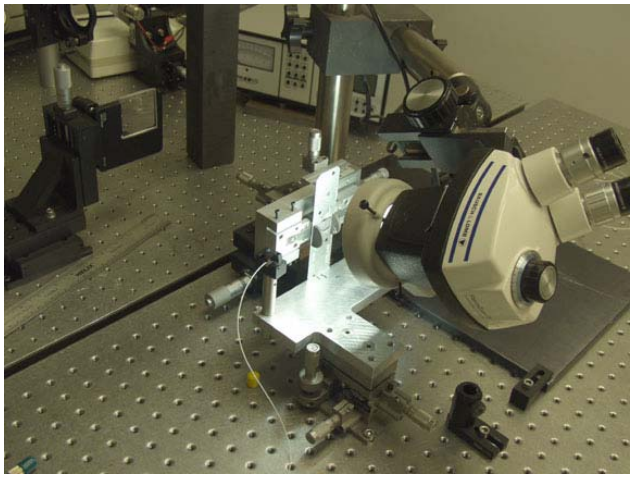

Figure 7. Set-up for exposing fiber to excimer laser output.

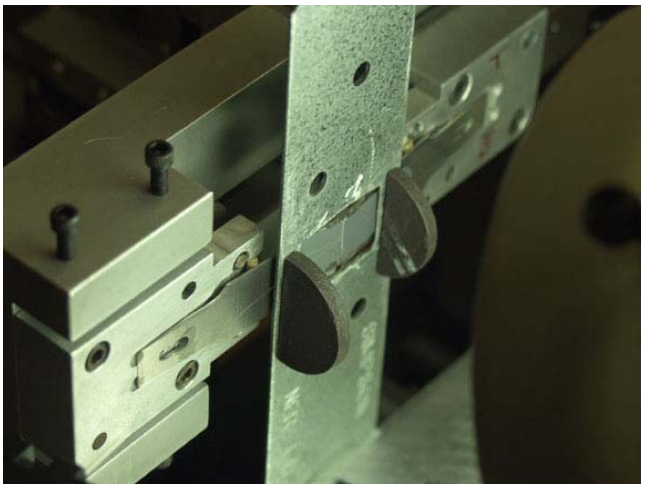

Figure 8. Close-up of set-up, showing silicon shutters used to define exposure aperture.

The Fabry-Perot interferometer sensor element is written in the optical fiber by exposing two sections of a photosensitive optical fiber to the output of an excimer (UV) laser to form two reflectors, which define a resonant optical cavity. When the light from the OTDR is injected into the input fiber, the two reflections interfere in the fiber, and are guided back to the end of the OTDR, where the state of interference may be analyzed using a photodetector. The state of interference (constructive or destructive) depends on the phase difference of the two reflections, which in turn is a function of the distance separating the fibers (the gap separation). If an acoustically generated strain is applied to the sensor, the separation of the reflectors is modulated.

Figure 9 shows a theoretical plot showing the output of an IFPI cavity over a wavelength range from 800 nm to 820 nm. The solid red curve corresponds to the spectral output of an IFPI with a cavity length of 40 μm, and blue dotted curve is for a cavity length of 42 μm. The two curves show that as the cavity length is increased, the waveform is shifted to the right (towards increasing wavelength).

In theory, the OTDR laser outputs light at a single wavelength, represented as the green line on the plot in Figure 9. Under that assumption, the OTDR output will vary as the change in cavity length causes the sensor's spectral output to shift. In reality, however, the laser output in the OTDR has a finite linewidth (spectral width), corresponding to a full-width, half-maximum of 10 nm. In Figure 9, this 10 nm FWHM spectral range is represented by the light yellow background. The output of the OTDR is the spectral response of the cavity integrated over the 10 nm FWHM range. Since more than one period of the sinusoid is integrated, the sensitivity of the sensor is reduced.

The solution to this problem is to fabricate IFPI cavities of shorter length. Figure 10 shows the theoretical spectral response of a 10 μm IFPI cavity, superimposed over the 10 nm FWHM of the laser centered at 813 nm. In this case, less than a full period of the sinusoid is integrated, with a result that OTDR output still varies with changing cavity length. Therefore, shorter IFPI cavity lengths are preferred for acoustic sensors.

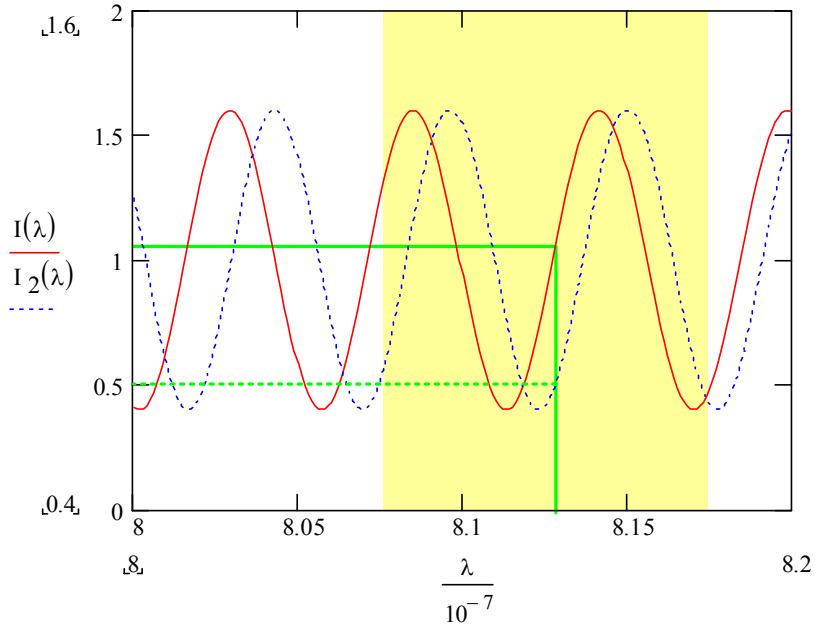

Figure 9. Spectrum for IFPI cavity over wavelength range from 800 to 820 nm. (Red curve is for a cavity length of 40 μm, and blue dotted curve is for a cavity length of 42 μm. The green line represents the light from a hypothetical OTDR laser at 813 nm).

IPFI cavities with cavity length less than 40 microns but greater than 20 microns were fabricated in our laboratory through the "dual-exposure" technique developed earlier in the program. This technique utilizes a 20 micron exposure at each end of the FP cavity. For FP cavities less than 40 microns this means that the two exposures overlap in the middle. Cavities with a length less than 20 microns can also be achieved but via a single exposure of appropriate length. However, these single exposure cavities have a reduced reflectivity when compared to the dual exposure variety. It is believed that the decreased reflectivity is due to the difficulty in matching reflectors when using a single exposure.

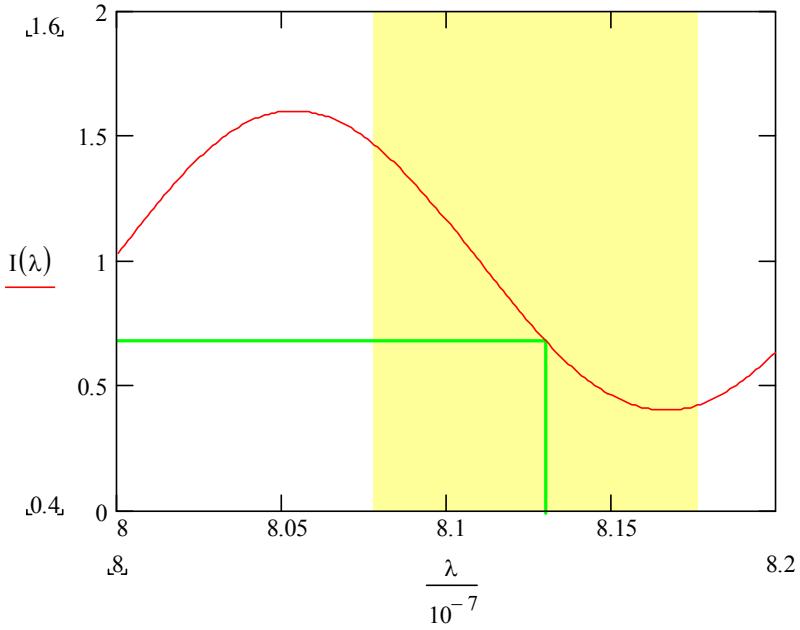

Figure 10. Spectrum for 10 μm IFPI cavity.

An investigation of methods for coupling of acoustic stress waves from a plate to the fiber optic sensor was undertaken. The goal was to couple acoustic emissions (stress waves) to changes in IFPI cavity length. In order to achieve maximum output from the sensor, the IFPI cavity would need to experience length changes of approximately 250 *nm*. Several packaging schemes were investigated in an effort to couple acoustic waves to IFPI cavity deformation.

The most simplistic approach was to bond the IFPI cavity to a silica substrate using a CTE compatible bonding agent; and then attach the substrate to the device under test, as shown in Figure 11. Evaluation of this design showed no response to acoustic emissions such as a pencil lead break test.

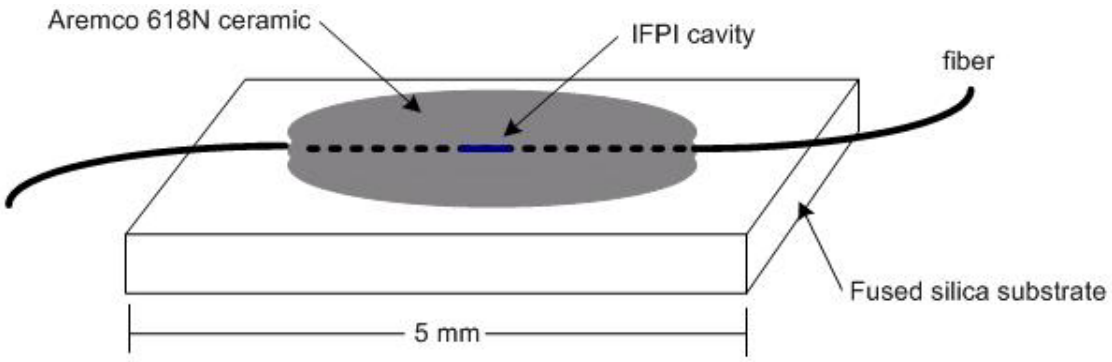

Figure 11. Illustration of IFPI sensor packaging.

Another approach was to bond the IFPI cavity across an air gap as shown below in Figure 12. This sensor is created by bonding two risers to the device under test, then bonding the fiber to the risers such that the IFPI cavity spans the air gap. The intention with this design was to maximize the force applied to the IFPI cavity due to stress waves in the device under test. Unfortunately, this design also showed little sensitivity to acoustic emissions.

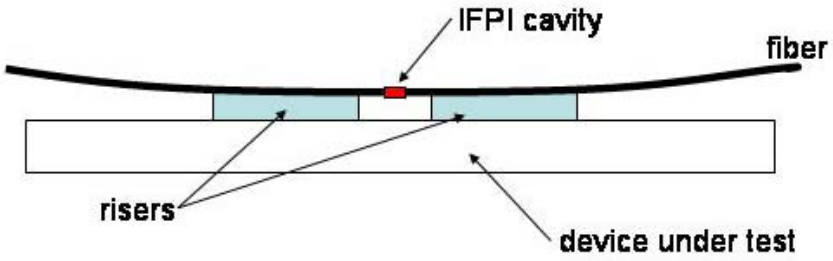

Figure12. Acoustic sensor configuration using an IFPI cavity.

The third approach was taken from the available literature concerning optical hydrophones. Such hydrophones are created by wrapping lengths of fiber around a metallic thin walled hollow cylinder and bonding the fiber to the cylinder. The cylinder acts as a large receiver; and the thin wall makes for large deflections and therefore better coupling to the optical sensor. The Figure 13 shown below is of such an acoustic sensor. The large metallic cylinder is seen to the left of the oscilloscope waveform. The IFPI fiber is epoxy bonded to the cylinder. This sensor showed better sensitivity to acoustic waves than any of the previous attempts, and was observed to respond to voices in close proximity to the cylinder. Overall, the sensitivity of this proof-of-concept design was reasonable and probably deserves further investigation.

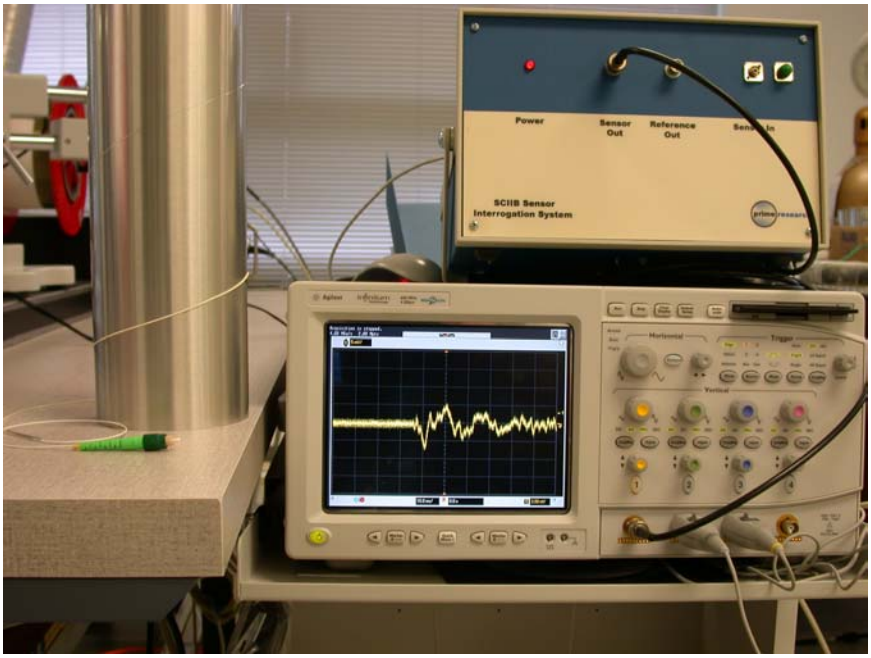

Figure 13. An acoustic sensor utilizing an IFPI transducer is shown to the left of the oscilloscope waveform. This design concept was the most sensitive of all the IFPI designs.

The difficulty in coupling acoustic waves to an IFPI cavity is believed to be related to the amount of force required to change the gap length by 250 *nm*. In the following sections, the reader will see that optical acoustic sensors were successfully produced but did not utilize IFPI cavities as the transducing element. Instead, the successful sensors utilized EFPS type configurations to transduce the acoustic waves. EFPS sensors are distinguished by there use of an air gap to form the FP cavity; whereas an IFPI has glass joining the two sides of the gap. Since the two sides of an EFPS cavity are separated by air (as opposed to glass for an IFPI); the force required to change the gap length by 250 nm can be small and tailored via the package design to suit the application.

An alternate fiber optic acoustic sensor design incorporates an air gap between the end of an optical fiber and an extra reflector; the fiber end and the reflector form a Fabry-Perot interferometric cavity, which is generally termed an extrinsic Fabry-Perot interferometer. As stress waves cause a change in the separation between the fiber in and the reflector, the interference signal between the two reflections is modulated, and can be related to the acoustic signal.

The packaging design employed for the extrinsic Fabry-Perot acoustic Sensor is shown in Figure 14, and is characterized by the metal housing, metal end-cap, ceramic base-plate, fiber-in-ferrule, rubber isolator, and a gold mirror. The fiber end-face is cleaved and positioned at 20 μm from the gold mirror to form a Fabry-Perot cavity. The acoustic waves cause the housing to deflect relative to the isolated fiber end-face, thereby changing the intensity of the Fabry-Perot interferometer. The cylindrical design can be

tuned per application by modifying geometric and material parameters, namely the rubber isolator material stiffness and dimensions.

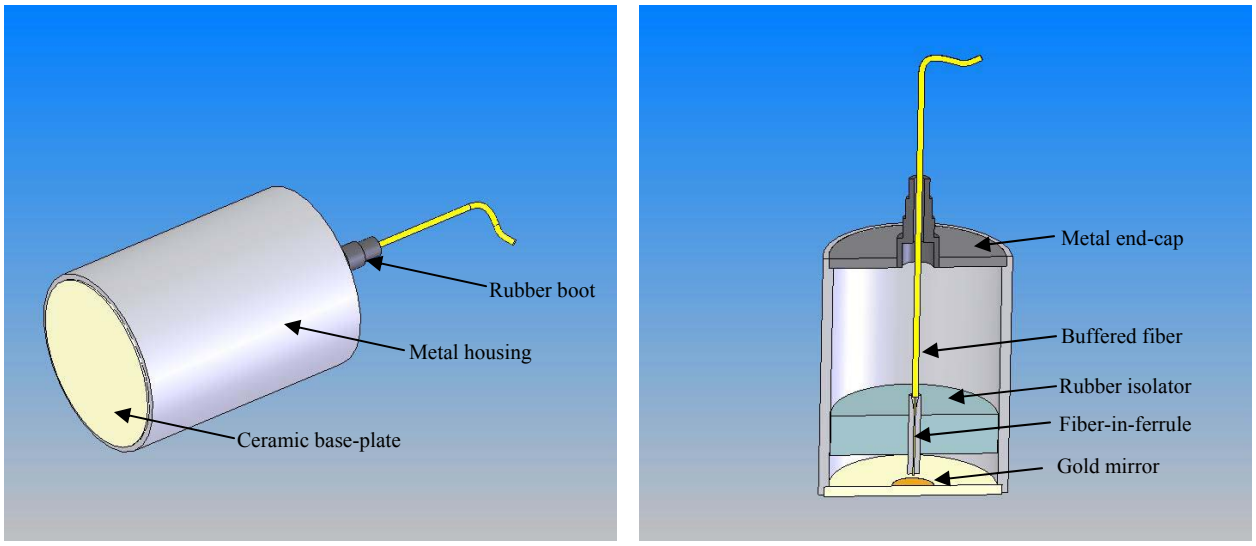

Figure14. Optical acoustic emission sensor packaged in a PAC standard housing.

A third sensor design investigated during the research is referred to as the "cantilever design" and is shown below in Figure 15. The cantilever design is composed of a silica substrate, silica pedestal, silica cantilever beam, a gold mirror reflector, and metallic housing. The optical fiber is bonded to the cantilever beam and the cleaved end face is located 20 µm from the gold mirror to form a Fabry-Perot cavity. The silica substrate is bonded to the surface of interest with a thin layer of adhesive. Acoustic waves cause the cantilever to deflect thereby changing the intensity of the Fabry-Perot interferometer.

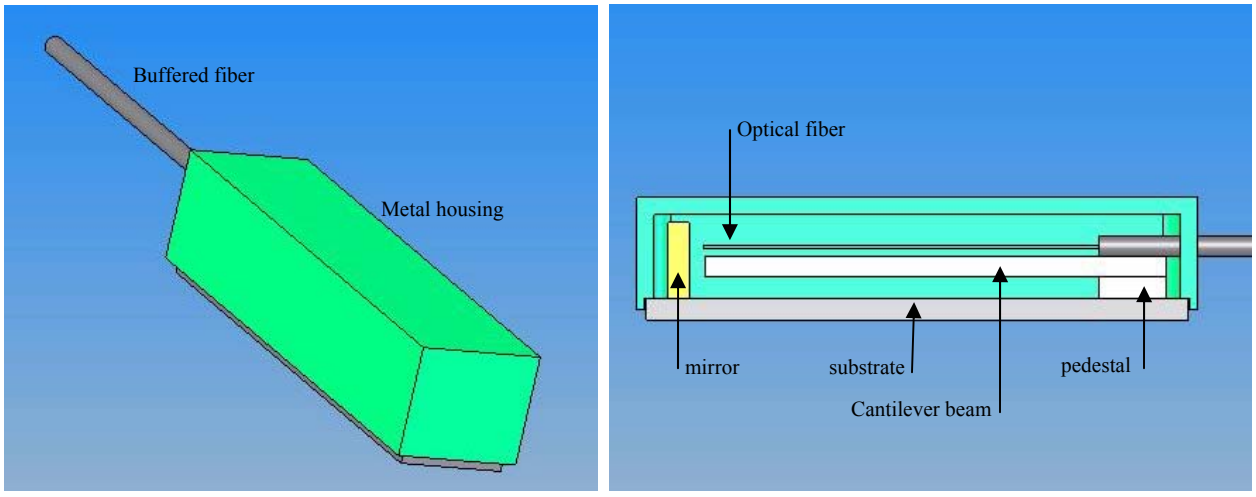

Figure15. Optical acoustic sensor cantilever design.

The dimensions of the cantilever beam (height, width, length) can be adjusted to provide a flat response and to avoid resonance over the frequency range of interest. Natural frequencies of a cantilever beam are given by the following equation:

$$\omega_r = \frac{(\lambda_r L)^2}{L^2} \frac{(EI)^{\frac{1}{2}}}{(\rho A)},$$

where

E is the material modulus of elasticity,
I is the beam cross-sectional moment of inertia,
ρ is the material density,
A is the beam cross-sectional area,
L is the beam length, and
λ_r and L are the roots of the characteristic equation, which is

$$\cos(\lambda L)\cosh(\lambda L) + 1 = 0 .$$

No simple expression for the roots of the characteristic equation is available so a numerical solution is required. The 1st four roots are found to be

$\lambda_1 L = 1.8751$
$\lambda_2 L = 4.6941$
$\lambda_3 L = 7.8548$
$\lambda_4 L = 10.996$

Using the above equations it is possible to tailor the dynamic response of the acoustic sensor to the requirements of the application.

3.3 Task 3: Adapt sensor decoding system

In the first series of tests of the acoustic sensors, the SCIIB signal processing system was employed to convert to the optical output of the sensor to electrical signal. A standard pencil break technique was employed to generate acoustic stress waves in a steel topped table.

3.3.1 Evaluation of acoustic sensors using SCIIB processor

The pencil break test performed here utilized the standards and methods provided for in ASTM Volume 03.03 E976-00, "Standard Guide for Determining the Reproducibility of Acoustic Emission Sensor Response". The pencil break test was performed at distances of one, three, six, and 8.5 feet from the optical AE sensor. All tests utilized the cylindrical design of Figure 14, and were performed on a steel topped optical table of dimension 8' x 4'. The plots below (Figures 16 through 18) show the sensor response as a function of time for these four distances.

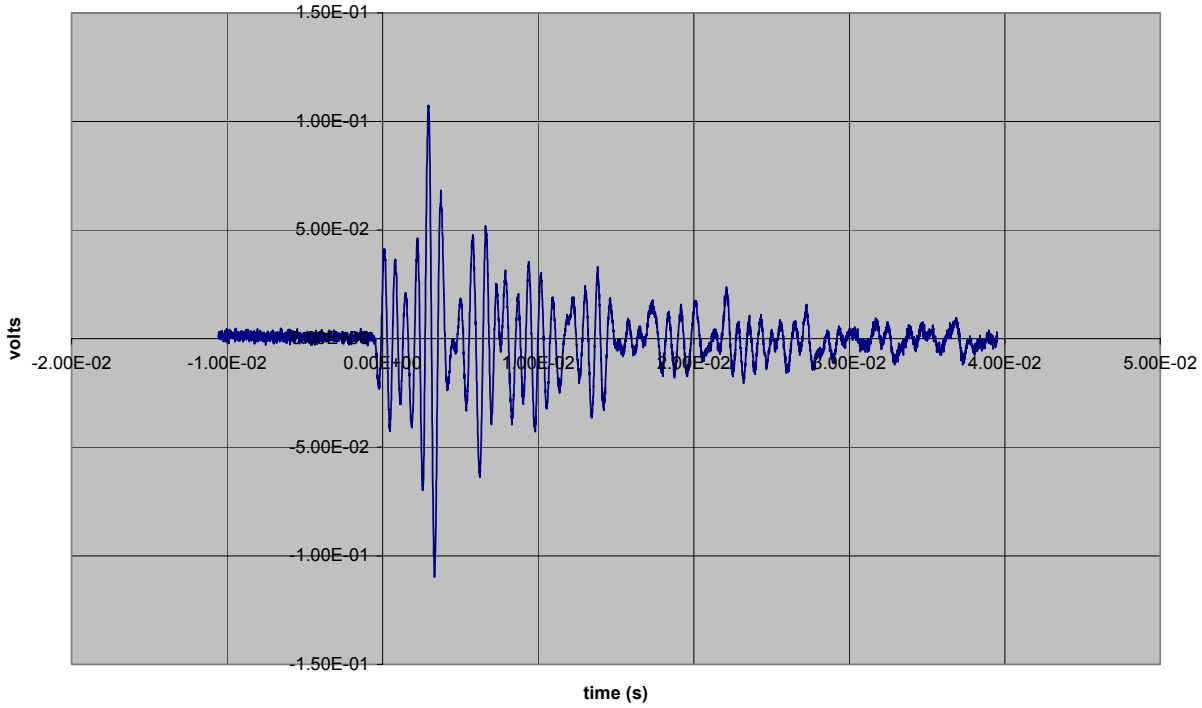

Figure 16. Response of the optical AE sensor to a 0.5 mm pencil lead broken at a distance of 1 ft.

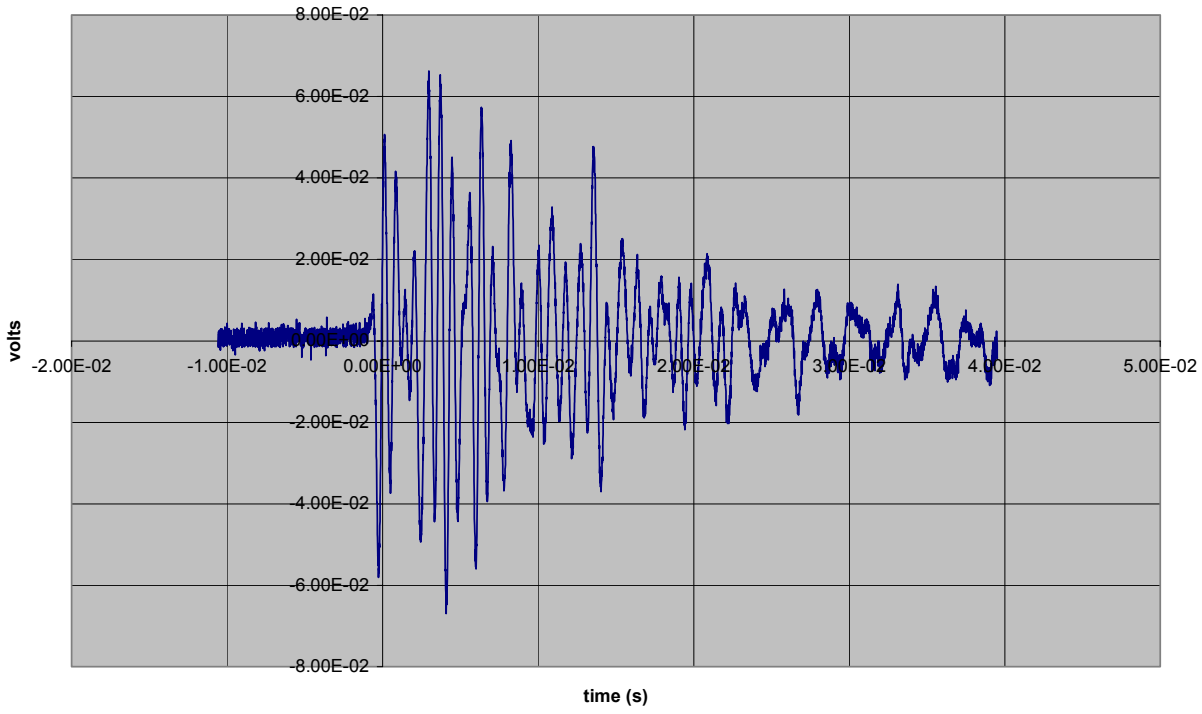

Figure 17. Response of the optical AE sensor to a 0.5 mm pencil lead broken at a distance of 3 ft.

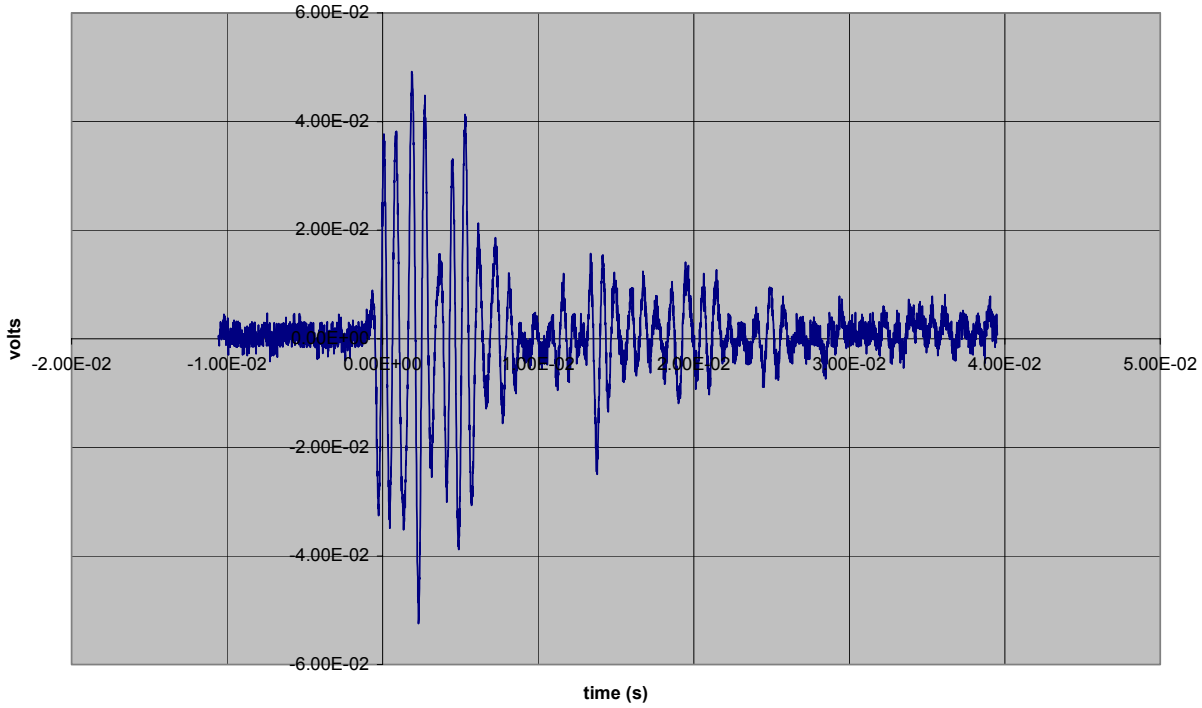

Figure 18. Response of the optical AE sensor to a 0.5 mm pencil lead broken at a distance of 6 ft.

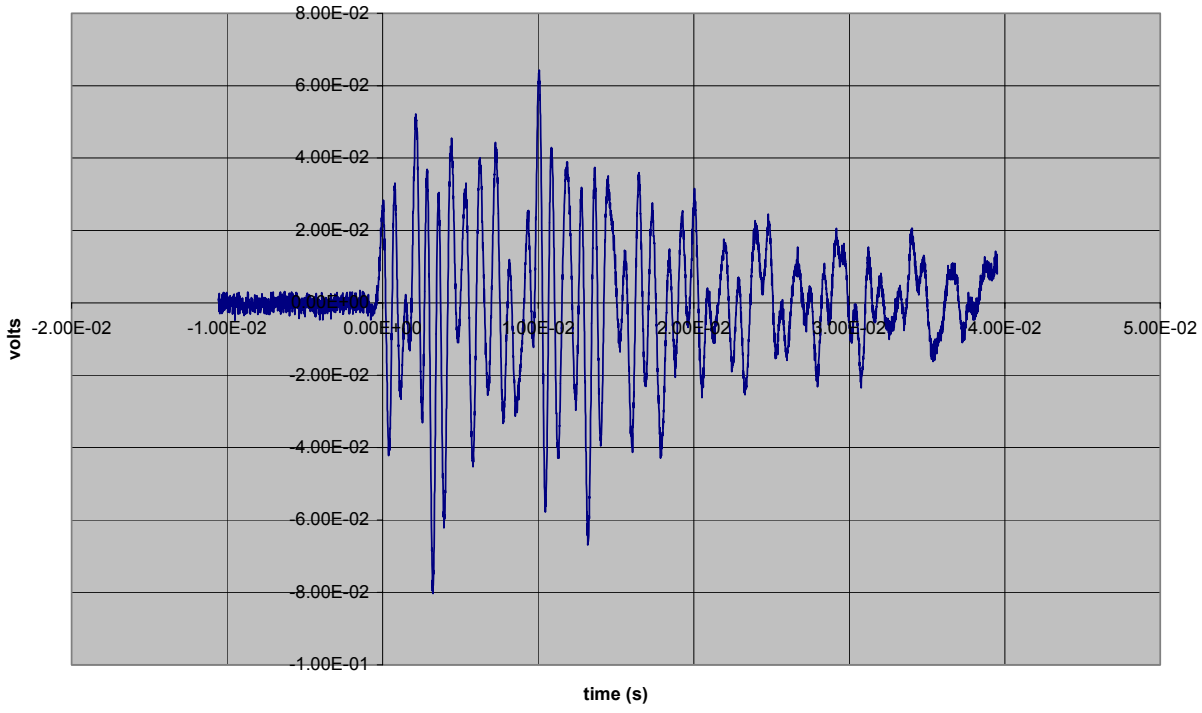

Figure 19. Response of the optical AE sensor to a 0.5 mm pencil lead broken at a distance of 8.5 ft.

3.3.2 Evaluation of sensors using an OTDR processor

In this section a comparison is made between two techniques for interrogating an IFPI temperature sensor. For ease of comparison, the same sensor was used for both interrogation trials. This IFPI sensor had a cavity length of 131 microns and was fabricated utilizing the methods described previously. The sensor was tested without any packaging and was not annealed previous to the trials.

The first test shown in Figure 20 utilized the Opto-Electronics OTDR for interrogation. A measurement using the OTDR is accomplished by measuring the return loss of the sensor relative to the return loss of Raleigh backscatter at a location just preceding the sensor. The purpose behind measurement of the Raleigh backscatter is to subtract out any return losses which occur before the sensor location. The OTDR allows the user to select the number of averages used for calculation of return loss, acceptable values range from 1 to 16383. The more averages the better the SNR, but at the expense of computation time. For instance; a return loss measurement using 128 averages takes approximately 27 seconds, 16383 averages takes 30 minutes. For this test the number of averages was set to 128.

In this OTDR test the oven temperature was taken from 50° C to 200° C in steps of 50° C, then allowed to cool back to 50° C and held at this temperature until conclusion of the test. It can be seen that the sensor responded to the 150° C temperature increase with a change in return loss of 0.2 dB. The noise amplitude is seen to be slightly less than 0.1 dB. The stability of the system can be observed for the remainder of the test as the temperature was maintained at 50° C. During this constant temperature the return loss can be seen to drift approximately 0.4 dB. These results are not encouraging and indicate a resolution of 75° C and very poor stability.

The next test shown in Figure 21 utilized a Micron Optics CTS tunable laser spectrometer for interrogation. By measuring the spectral (wavelength) response of a Fabry-Perot cavity by a spectrometer, the cavity length of the sensor can be determined; more exactly, by monitoring the spectral response of the sensor, a change in the phase of the interferometric signal resulting from an applied measurand can be measured. For this test the oven temperature was taken from 50° C to 200° C in steps of 50° C, then allowed to cool back to 50° C and held at this temperature until conclusion of the test. It can be seen that the sensor responded to the 150° C temperature increase with a change in phase of 1.2 radians. The noise amplitude is seen to be approximately 0.02 radians. The stability of the system can be observed for the portion of the test where the temperature was maintained at 50° C. During this constant temperature the phase does not have any noticeable drift. These results indicate a resolution of approximately 2.5° C, much better than the 75° C resolution of the OTDR.

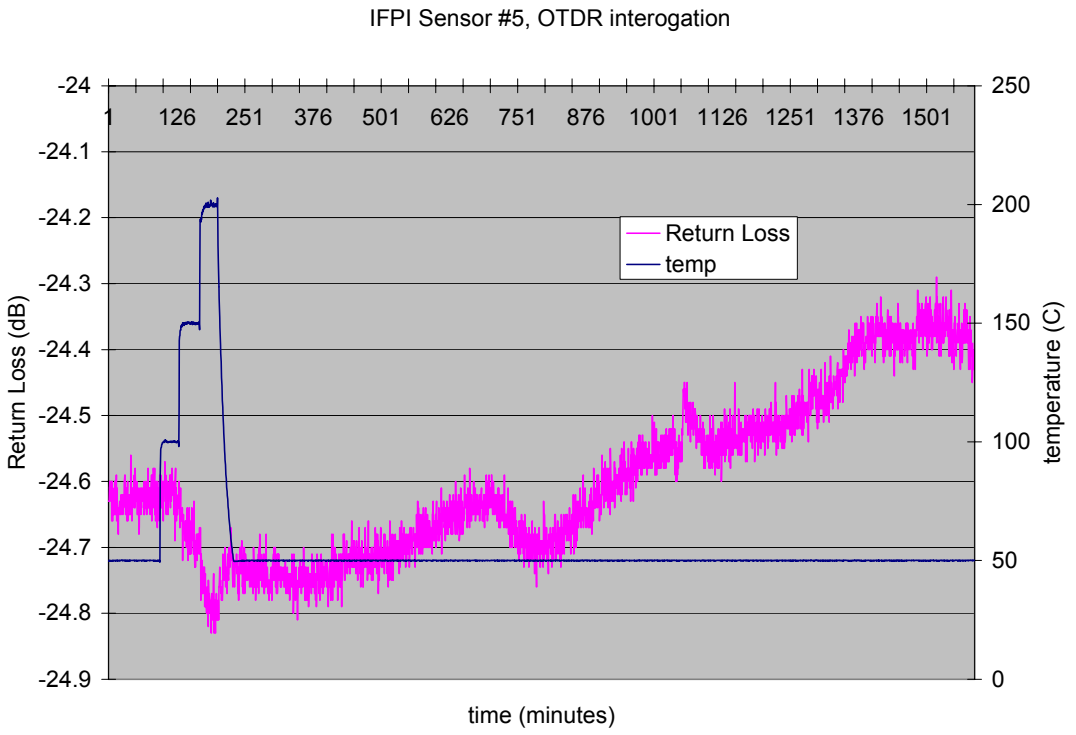

Figure 20. OTDR interrogation of an IFPI temperature sensor. The plot shows the sensor response (return loss) and the oven temperature as a function of time.

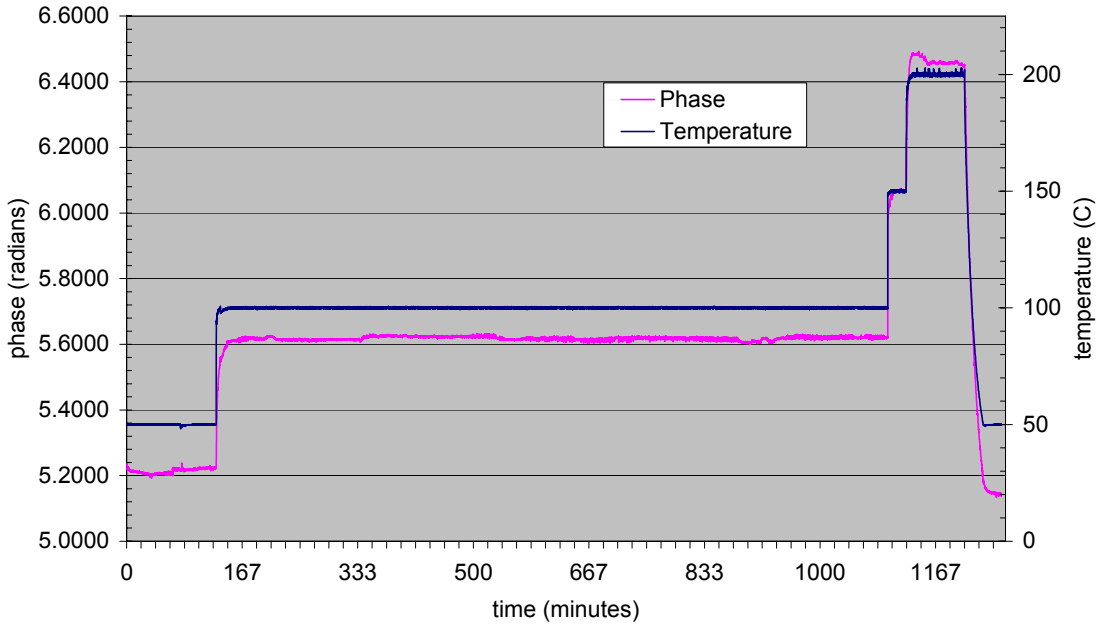

Figure 21. CTS interrogation of an IFPI temperature sensor. The plot shows the sensor response (phase) and the oven temperature as a function of time.

Another limitation in the application of OTDR for multiplexing Fabry-Perot sensors on a single fiber was found to result from multiple reflections between two or more sensors within the fiber. The simplest case, in which two sensors are multiplexed on a single fiber, is illustrated graphically in Figure 22. The blue line illustrates the path that a light pulse injected into the input of the fiber takes as it propagates through the fiber. One reflection is generated by Sensor 1; this reflection propagates back to the fiber to the OTDR, where it is detected as a light pulse, and a distance to Sensor 1 is determined by the time it took the pulse to travel out and back. The remaining light travels on to Sensor 2, which generates a second reflection. Most of that reflection propagates back to the OTDR, but some fraction of that second reflection generates a forward propagating reflection when it encounters Sensor 1.

When this forward propagating reflection reaches Sensor 2, yet another reflection is generated, this one propagating back to the fiber to the OTDR. This reflection will be detected a the OTDR as a pulse corresponding to a nonexistent sensor in the fiber, with a distance from the OTDR given by the distance that the light pulse traveled through its multiple reflections. This spurious signal has been termed a "ghost" by the OTDR as manufacturer, in reference to the fact that the multiple reflections generate an apparition of a signal. Since the power in each reflection is only a small fraction of the power in the pulse incident on each sensor (typically the reflected power is over 20 dB down from the incident power), the ghost is always lower in power than the valid sensor signals. Higher order ghosts, resulting from even more reflections, may be observed, but at greatly attenuated amplitudes. The number of possible ghosts increases exponentially with the number of sensors in the fiber.

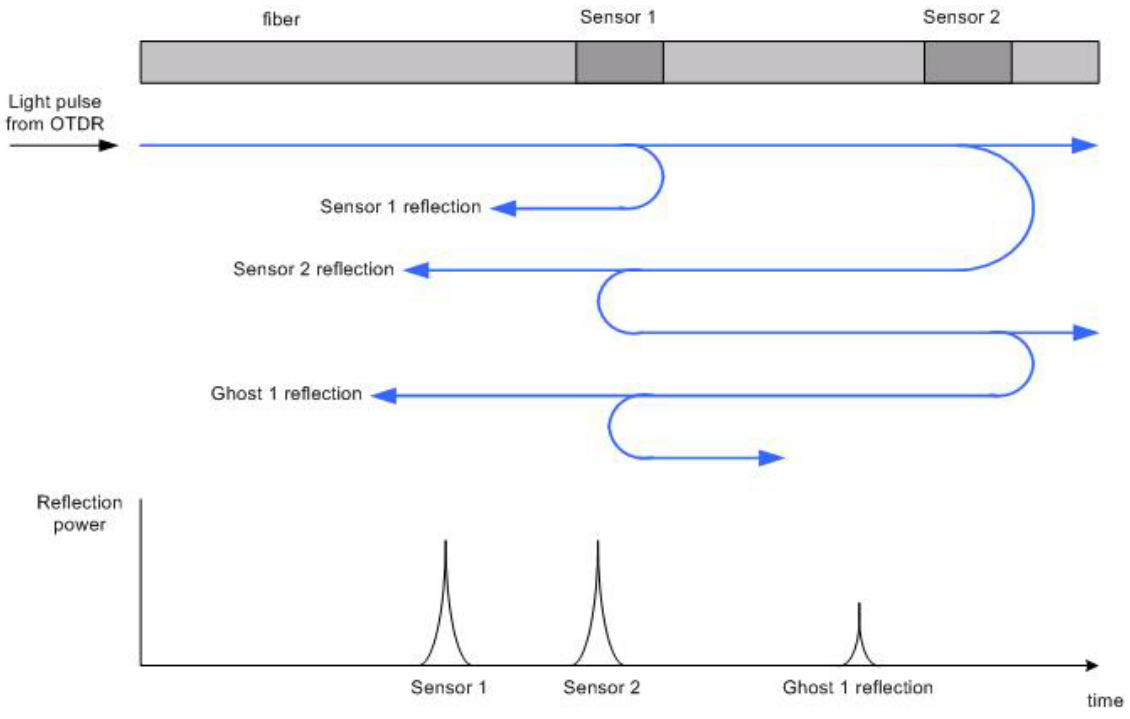

Figure 22. Illustration of ghost reflections in OTDR systems.

If the location of every sensor in the fiber is known, the location of every ghost in the OTDR output can be predicted. In the example shown in the figure, the Ghost 1 signal lags in time the Sensor 2 signal by the amount of time that it takes the pulse to travel the distance between Sensor 1 and Sensor 2 twice. Since the refractive index of the fiber core is well known, this is a straightforward calculation. For more complex situations involving multiple sensors, a computer could be programmed to calculate the location of the ghost signals, and to ignore the signals.

A similar program could be used to optimize the location of the sensors along the fiber, to guarantee that no ghosts overlap a valid reflection signal from an existing sensor.

3.4 Task 4: Determine sensitivity of fiber optic system using acoustic standards

The experimental results illustrated in Section 4.3.1, in which acoustic stress waves were generated using a standardized ASTM Volume 03.03 E976-00 method, provide a qualitative measure of the extrinsic Fabry-Perot acoustic sensor sensitivity. The sensitivity of the fiber optic sensor could not be determined due to a lack of a calibrated reference acoustic sensor. According to the cited ASTM standard, "The absolute calibration of a sensor requires complete knowledge of the characteristics of the acoustic wave exciting the sensor or a previously calibrated reference sensor." However, although the amplitude of the acoustic wave is not known in this case, the ASTM standard provides for a reproducible acoustic wave which can be used to compare the relative merits of different sensors. Again, according to the standard, "This guide provides simple economic procedures for testing or comparing the performance of acoustic emission sensors. These procedures allow the user to check for degradation of a sensor or to select sets of sensors with nearly identical performances."

From a series of tests performed using acoustic wave is generated by the standardized tensile break excitation, it was clear that the extrinsic Fabry-Perot sensor was much more sensitive than the IFPI sensor design.

3.5 Task 5: Design sensor network

It was determined during the investigation that OTDR-based interrogation is not well suited for monitoring of acoustic signals, due to the limited bandwidth of the OTDR system. This is in large part a consequence of the fact that the OTDR is a time-domain method in which one output (position of the sensor on the fiber) is encoded as a variable of time (specifically, the time the flight of a pulse from the OTDR to the sensor and back). In order to simplify the correlation of reflected pulses with specific sensors on the fiber, the pulse repetition rate of the OTDR's laser is adjusted so that once a pulse of light is launched into the fiber, another pulse is not generated by the laser until the first pulse has traveled to the for the sensor and returned to the OTDR. Therefore, the longer the fiber, the longer the laser must wait for a pulse to reflect before generating another pulse. For the Opto-electronics OFM-20 high resolution OTDR used for the study, the pulse

repetition rate is a maximum of 1 MHz for short fibers, and less for longer fibers. Since light travels of the speed of approximately 1 foot per nanosecond in optical fiber, it will take about 100 μs for the light to travel to the end of a 10 mile fiber and back. So for a 10 mile fiber, the maximum permissible pulse repetition rate is approximately 10 kHz. Since each pulse output by the laser has a very short duration (< 1 ns), each pulse can be considered to be one sample in time of the acoustic signal at a particular sensor. Using the Nyquist Criterion from digital signal processing theory, the maximum bandwidth of a signal that can be reconstructed from a 10 kilosample per second sampling rate is 5 kHz. This predicted maximum signal bandwidth is significantly less than the 40 kHz identified as the requirement for detection of pipeline leaks, as reported in Section 4.2 above.

A further penalty on signal bandwidth is imposed by the need to use averaging to obtain acceptable signal-to-noise ratios (SNR). In order to improve the SNR, multiple reflections are added and averaged. For a dynamic range of less than 75 dB, the accuracy of the OTDR system in determining the amplitude of reflected signal is ±0.5 dB if 32 averages are employed. Typically, this averaging process will require approximately 5 seconds per sensor. An accuracy of ±0.1 dB may be obtained by increasing the averaging time to 60 seconds per sensor (which would result in a signal bandwidth of about 0.01 Hz.

4 Estimates of technical feasibility

The results obtained during this Phase I research effort suggests that the IFPI/OTDR sensor system proposed as a means for gas pipeline monitoring and leak detection is not feasible for this application. The reasons for this assessment include:

1. The high Young's modulus of the all-glass IFPI sensor results in a stiff assembly, which makes coupling of acoustic waves from the pipe into the sensor difficult.
2. The large amplitude of noise in the OTDR system limits the achievable resolution of an OTDR-based system.
3. The maximum repetition rate of the OTDR laser (which is determined by the length of the interrogated fiber) and the need to average and returned signal in order to improve SNR limits of the maximum the taxable bandwidth of the acoustic signal to a value much less than that required for detection of pipeline leaks.
4. Spurious signals (ghosts) caused by multiple reflections between sensors in the fiber imposed constraints on the location of sensors along the fiber, and increase processing required to extract the acoustic signal.

Investigation of alternate sensor designs and interrogation techniques suggest the following alternatives may be applicable to pipeline monitoring:

1. Much higher sensitivities to acoustic signals were observed using a Fabry-Perot sensor with an air gap cavity (extrinsic Fabry-Perot sensor), due to the reduced stiffness of the sensor assembly.
2. The SCIIB interrogation system were shown to result in much higher signal-to-noise ratios than those possible with the OTDR system. However, the SCIIB system is not easily extended to interrogation of serially multiplexed sensors. Coherence multiplexing, in combination with the SCIIB self-calibration features, is one possible way to extend the SCIIB system to use with more than one sensor.

Development of methods for manufacturing of IFPI sensors to the use of a UV laser was very successful, with significant improvements in the quality of the sensors fabricated over the course of the program. While the mechanical properties of the IFPI sensors make them poorly suited for acoustic sensors, the experimental results show that they function very well as temperature sensors.